

## Project closing report - FK129094

### Experimental investigation of the pathomechanisms of radiation-induced heart disease: the role of microRNAs

#### 1. Summary of the original commitments:

The original commitments of the present project were the following:

- 1) Set-up of *rodent models* of acute and chronic radiation-induced heart disease (RIHD) in males;
- 2) investigation of the effects of selective heart irradiation on the expression of cardiac and/or circulating *miRs and/or mRNAs* in both the acute and chronic models of RIHD;
- 3) investigation of effects of *preimplantation factor (PIF)* on RIHD and RIHD-associated cardiac expression changes of selected miRs and mRNAs in both the acute and chronic models of RIHD;
- 4) identification of potential *miRs and genes for diagnostic marker and therapeutic target development in RIHD*;
- 5) investigation of *molecular mechanisms* by which selected miRs or PIF treatment can influence the cardiac gene expression profile in RIHD.

#### 2. Summary of additional experiments and results beyond the project's original commitments:

1. Investigation of the effects of selective heart irradiation on *proteomic alterations* in both the acute and chronic models of RIHD;
2. investigation of *the effects of PIF on RIHD in female rats* (we used a lower radiation dose [12 Gy vs. 50 Gy] and longer follow-up time [9-10 months vs. 15-19 weeks] in the chronic female model of RIHD compared to males; this side project is in progress);
3. investigation of *the effects of PIF on human breast cancer cell lines and human ventricular cardiac fibroblasts* in collaboration with other research groups;
4. investigation of the effects of the angiotensin-II receptor blocker *losartan on RIHD* and RIHD-associated cardiac expression changes of selected miRs and mRNAs in both the acute and chronic models of RIHD;
5. investigation of the effects of *losartan and the  $\beta$ 3-adrenoceptor agonist mirabegron on cardiotoxic effects and heart failure induced by doxorubicin*, which is a commonly used chemotherapeutic agent in combination with radiotherapy;
6. the investigation of the effects of *losartan and mirabegron in another heart failure model, i.e., uremic cardiomyopathy* in rats.

#### 3. Published articles and PhD thesis defenses during the supportive period of the project

*Originally, at the end of the project, 3-4 publications in international, high-rank, peer-reviewed journals and 1 PhD thesis defense were anticipated. These endpoint commitments have been fulfilled during the project:*

##### 3.1. Published articles strongly linked to the topics of the present project:

1. Márta Sárközy, Renáta Gáspár, Ágnes Zvara, Laura Kiscsatári, Zoltán Varga, Bence Kóvári, Mónika Gabriella Kovács, Gergő Szűcs, Gabriella Fábrián, Gábor Cserni, László G. Puskás, Thomas Thum, Zsuzsanna Kahán, Tamás Csont, Sándor Bátkai. *Selective heart irradiation induces cardiac overexpression of the pro-hypertrophic miR-212*. **FRONTIERS IN ONCOLOGY**. 9:598; 2019 (Q1, IF: 4.137), doi: 10.3389/fonc.2019.00598

2. Márta Sárközy, Zoltán Varga, Renáta Gáspár, Gergő Szűcs, Mónika G. Kovács, Zsuzsanna Z. A. Kovács, László Dux, Zsuzsanna Kahán, Tamás Csont: *Pathomechanisms and therapeutic opportunities in radiation-induced heart disease: from bench to bedside*. **CLINICAL RESEARCH IN CARDIOLOGY** 110: (4) pp. 507-531., 2021 (D1, IF: 6.138), doi: 10.1007/s00392-021-01809-y
3. Mónika Gabriella Kovács, Zsuzsanna Z. A. Kovács, Zoltán Varga, Gergő Szűcs, Marah Freiwan, Katalin Farkas, Bence Kővári, Gábor Cserni, András Kriston, Ferenc Kovács, Péter Horváth, Imre Földesi, Tamás Csont, Zsuzsanna Kahán, Márta Sárközy. *Investigation of the Antihypertrophic and Antifibrotic Effects of Losartan in a Rat Model of Radiation-Induced Heart Disease*. **INTERNATIONAL JOURNAL OF MOLECULAR SCIENCES** 22(23):12963, 2021 (D1, IF: 6.208), doi: 10.3390/ijms222312963
4. Marah Freiwan, Gergő Szűcs, Zsuzsanna Z.A. Kovács, Mónika Gabriella Kovács, Réka Losonczy, Andrea Sója, Hoa Dinh, Gábor Cserni, András Kriston, Ferenc Kovács, Péter Horváth, Tamás Csont, László Dux, Márta Sárközy. *The effect of losartan, mirabegron and their combination on the development of doxorubicin-induced chronic cardiotoxicity in a rat model*. **INTERNATIONAL JOURNAL OF MOLECULAR SCIENCES** 23(4):2201, 2022 (D1, IF: 5.6). doi: 10.3390/ijms23042201

3.2. Published articles linked to the topics of the present project in a broader sense (investigating the same miRs or drugs in another heart failure model, i.e., uremic cardiomyopathy):

1. Zsuzsanna Z.A. Kovács, Gergő Szűcs, Marah Freiwan, Monika G. Kovács, Fanni M. Márványkövi, Hoa Dinh, Andrea Siska, Katalin Farkas, Ferenc Kovács, András Kriston, Péter Horváth, Bence Kővári, Bálint Gábor Cserni, Gábor Cserni, Imre Földesi, Tamás Csont, Márta Sárközy. *Comparison of the anti-remodeling effects of losartan and mirabegron in a rat model of uremic cardiomyopathy*. **SCIENTIFIC REPORTS** 2021 11(1):17495, 2021 (D1, IF: 4.996). doi: 10.1038/s41598-021-96815-5

3.3. Other published articles with the current NKFI grant ID (RT-qPCR primers, antibodies, or other consumables were shared with the abovementioned projects in 1.3.1. and 1.3.2.):

1. Márta Sárközy, Fanni Márványkövi, Gergő Szűcs, Zsuzsanna Z.A. Kovács, Márton R. Szabó, Renáta Gáspár, Andrea Siksa, Bence Kővári, Gábor Cserni, Imre Földesi, Tamás Csont. *Ischemic preconditioning protects against ischemia-reperfusion injury in chronic kidney disease in both males and females*. **BIOLOGY OF SEX DIFFERENCES**. 12:49, 2021 (D1, IF: 8.811). doi: <https://doi.org/10.1186/s13293-021-00392-1>
2. Márta Sárközy, Simon Watzinger, Zsuzsanna Kovács, Eylem Acar, Fanni Márványkövi, Gergő Szűcs, Gülsüm Lauber, Andrea Siska, Zsolt Galla, Imre Földesi, Attila Fintha, Andras Kriston, Ferenc Kovacs, Péter Horváth, Bence Kővári, Gábor Cserni, Tibor Krenács, Petra Szabó, Gábor Szabó, Péter Monostori, Karin Zins, Dietmar Abraham, Tamás Csont, Peter Pokreisz, Bruno K. Podesser, Attila Kiss. *Neuregulin-1 $\beta$  improves uremic cardiomyopathy and renal dysfunction in rats*. **JACC: BASIC TO TRANSLATIONAL SCIENCE** 8:1160–1176, 2023 (D1, IF: 9.531\*). doi: 10.1016/j.jacbts.2023.03.003
3. Hoa Dinh, Zsuzsanna Z.A. Kovács, Fanni Márványkövi, Merse Kis, Klaudia Kupecz, Gergő Szűcs, Marah Freiwan, Gülsüm Yılmaz Lauber, Eylem Acar, Andrea Siska, Katalin Eszter Ibos, Éva Bodnár, András Kriston, Ferenc Kovács, Péter Horváth, Imre Földesi, Gábor Cserni, Bruno K. Podesser, Peter Pokreisz, Attila Kiss, László Dux, Krisztina Csabafi, Márta Sárközy. *The*

*kisspeptin-1 receptor antagonist peptide-234 accelerates the development of uremic cardiomyopathy in a rat model. SCIENTIFIC REPORTS. 13:14046, 2023. (D1, IF: 4.996\*). doi: 10.1038/s41598-023-41037-0*

4. Tóth ME, Sárközy M, Szűcs G, Dukay B, Hajdu P, Zvara Á, Puskás LG, Szebeni GJ, Ruppert Z, Csonka C, Kovács F, Kriston A, Horváth P, Kővári B, Cserni G, Csont T, Sántha M. Exercise training worsens cardiac performance in males but does not change ejection fraction and improves hypertrophy in females in a mouse model of metabolic syndrome. **BIOLOGY OF SEX DIFFERENCES** 13:5, 2022 (D1, IF:8.811). doi: 10.1186/s13293-022-00414-6

#### 3.4. PhD thesis defenses:

1. **Dr. Mónika Gabriella Kovács** (100%) – *Investigation of the pathomechanism and potential therapeutic targets in radiation-induced heart disease in a rat model.* (2022, „Pro Laudanda Promotione” Prize) - <https://doktori.hu/index.php?menuid=193&vid=24552&lang=EN>
2. **Marah Muwaffaq Ibrahim Freiwan** (50%), - *Investigation of the antiremodeling effects of losartan, mirabegron and their combination on the development of doxorubicin-induced chronic cardiotoxicity in a rat model* (2022) - <https://doktori.hu/index.php?menuid=193&lang=EN&vid=24755>
3. **Dr. Zsuzsanna Kovács** (100%) – *Comparison of the antiremodeling effects of losartan and mirabegron in a rat model of uremic cardiomyopathy* (2021) - <https://doktori.hu/index.php?menuid=193&lang=EN&vid=23984>
4. **Dr. Fanni Magdolna Márványkövi** (100%), - *Investigation of the pathomechanism of uremic cardiomyopathy and the infarct size-limiting effect of ischemic preconditioning in a rat model of chronic kidney disease* (2023) - <https://doktori.hu/index.php?menuid=193&lang=EN&vid=26406>

## 4. Detailed results of the present project

### *4.1. Set up and characterization of acute and chronic models of RIHD in rats (Task 1/A)*

For the set-up of *in vivo* acute (24-h, 1-week, and 3-week follow-up [FUP] times) and chronic (15- and 19-week FUP times) models of RIHD, male Sprague-Dawley rats were divided into 2 groups in every FUP time point: 1) control and 2) radiotherapy (RT) with selective heart irradiation with a single dose of 50 Gy. Before the irradiation, cardiac function, and morphology were assessed by transthoracic echocardiography. PIF treatment was started on the day of the RT. In the chronic model of RIHD, transthoracic echocardiography was performed at weeks 6 and 12 to assess the severity of left ventricular hypertrophy (LVH) and diastolic dysfunction. Endpoint echocardiography was performed at weeks 1 and 3 in the acute models and at week 15 in the chronic model of RIHD to monitor cardiac function and morphology. Blood samples were collected at the end of FUP time, and hearts, lungs, and tibias were also isolated. Then, the hearts were separated into left and right ventricles. Samples of both ventricles were collected for histology and biochemical measurements (RT-qPCR, Western blot, next-generation sequencing [NGS], and proteomics).

Initially, the detailed molecular characterization of two RIHD models (*i.e.*, 1-week and 19-week FUP times) was the aim of the current project, and the other three RIHD models (*i.e.*, 24-h, 3- and 15-week FUP time models) was beyond the commitments of the original project plan. However, we also aimed to detect the early acute (*i.e.*, 24 h FUP time, without significant cardiac functional and morphologic differences), the subacute (*i.e.*, 3-weeks FUP time with mild left ventricular hypertrophy), and the early chronic (*i.e.*, 15-weeks FUP time with left ventricular hypertrophy and mild fibrosis)

molecular changes. Our 19 weeks FUP time RIHD model with severe concentric left ventricular hypertrophy and interstitial fibrosis was previously characterized by echocardiography and several molecular markers (Kiscsatári *et al.*, In vivo, 2016)

In the present project, in the 1-week FUP time RIHD model, body weight and tibia length were not significantly different from the control group. The red blood cell count was significantly increased in the RT group compared to the control group, suggesting the presence of a radiation-induced lung injury and acute hypoxia, which might be compensated by increased red blood cell count. The white blood cell count failed to increase in the RT group compared to the control group. The echocardiographic measurements showed the development of diastolic dysfunction and increased heart rate in the RT group compared to the control group. The LV ratio of collagen-1a1 to collagen-3a1 (*Col1a1/Col3a1*, an indicator of fibrosis development) and the expressions of the atrial natriuretic peptide (*Nppa*, considered as a cardiac stretch marker) and the inflammatory marker interleukin-1 (*Il1*) were significantly increased in the RT group as compared to the control. The LV expressions of other inflammatory markers, *i.e.*, interleukin-6 (*Il6*) and tumor necrosis factor-alpha (*Tnf*), showed a trend toward an increase in response to RT as compared to the control (Kovács MG *et al.*, Int. J. Mol. Sci., 2021, <https://doi.org/10.3390/ijms222312963>).

In the 3-week FUP time RIHD model, the body weight was significantly lower in the RT group compared to the control. The left ventricular weight was significantly decreased in the RT group compared to the control group. The lung weight was significantly increased in the RT group compared to the control group, indicating the presence of lung edema in RIHD. Despite the radiation-induced lung injury and secondary hypoxia, the red blood cell count failed to elevate in the RT group. In contrast, the white blood cell count was significantly increased in the RT group, indicating the presence of systemic inflammation. Based on the echocardiographic data, posterior and inferior wall thicknesses were significantly increased, and the left ventricular end-systolic and end-diastolic diameters were significantly decreased in the RT group compared to the control group, pointing out the development of a mild LVH. The left ventricular expressions of the connective tissue growth factor (*Ctgf*, a fibrotic marker), the ratio of the beta-myosin heavy chain to the alpha-myosin heavy chain (*Myh7/Myh6*, used as an LV hypertrophy and tissue hypoxia marker), matrix metalloprotease-2 (*Mmp2*, a marker associated with cardiac remodeling), angiotensinogen (*Agt*), the angiotensin-II type 2 (AT2)-receptor at the protein level, and the pro-inflammatory *Il1*, *Il6*, and *Tnf* were significantly increased in the RT group as compared to the control. *Nppa* expression showed a trend toward an increase in response to RT as compared to the control group (Kovács MG *et al.*, Int. J. Mol. Sci., 2021, <https://doi.org/10.3390/ijms222312963>).

In the 15-week FUP-time RIHD model, the body weight was significantly decreased in the RIHD group compared to the control group from week 2 to the end of the FUP time. The tibia length and the heart weight were significantly reduced in the RT group compared to the control group, indicating the smaller size of the irradiated animals. In contrast, the lung weight was not significantly different in the RT group compared to the control group, indicating lung edema in chronic RIHD. In accordance with this hypothesis, red blood cell count, hemoglobin, and hematocrit values were significantly increased in the RT group, indicating the presence of a compensatory mechanism in response to chronic hypoxia potentially caused by radiation-induced lung injury, fibrosis, and edema. The anterior, inferior, posterior, and septal wall thicknesses were significantly increased, and the left ventricular end-systolic and end-diastolic diameters were significantly decreased with a markedly increased E/e' ratio in the RT group as compared to the control group, indicating the development of severe concentric LVH and diastolic dysfunction. The LV expressions of *Ctgf*, *Myh7/Myh6* ratio, *Mmp2*, *Nppa*, B-type natriuretic peptide (*Nppb*), the pro-hypertrophic and fibrotic STAT3, chymase (*Cma*, alternative activator of the renin-angiotensin-aldosterone system in tissues), plasminogen (*Plg*, another alternative activator of the renin-angiotensin-aldosterone system in tissues), the pro-inflammatory *Il6*, and the anti-inflammatory *Il10* were significantly increased; and the immunomodulatory interferon- $\gamma$  (*Ifng*) and the apoptosis- and autophagy-associated mTOR were significantly decreased in the RT group

as compared to the control. In the RIHD group, histology validated significant LV interstitial fibrosis (Kovács MG *et al.*, Int. J. Mol. Sci., 2021, <https://doi.org/10.3390/ijms222312963>).

In summary, our chronic RIHD models reflect most of the echocardiographic and molecular changes of real-life RIHD patients; therefore, our models seem to be appropriate for performing translational studies and testing new pharmacologic agents (Bergom *et al.*, JACC: CardioOncology, 2021, 3:343–359, <https://doi.org/10.1016/j.jacc.2021.06.007>).

#### **4.2. Exploring novel pathomechanisms of RIHD and identification of possible new therapeutic targets and identification of early circulating diagnostic markers of RIHD (Task 1/B and Task 2)**

Bioinformatics analysis of next-generation sequencing (NGS, n=3 in each group in each FUP time point) for miRs and mRNAs as well as proteomics (n=6 in each group in each FUP time point, beyond the scope of the original project plan) in the LV samples of 24-h, 1-, 3-, 15- and 19-week FUP times RIHD models are finished. The proteomic measurements and data analysis were performed in collaboration with Dr. Zoltán Szabó and Bella Bruszel in the Dept. of Medical Chemistry, Albert Szent-Györgyi Medical School, Univ. of Szeged.

KEGG, GO, and Reactome pathway analyses are also done for the significantly changed mRNAs in all RIHD models. Potential miR and mRNA target pairs were also identified by *in silico* models (*e.g.*, matching the significantly up-regulated miRs and down-regulated mRNAs and significantly down-regulated miRs and up-regulated mRNAs). miR and gene expression changes were considered significant if the adjusted p-value < 0.05 and the log fold change value < -1 (down-regulation) or > 1 (up-regulation) or the fold change value < - 2 (down-regulation) or > 2 (up-regulation). Selected NGS and RT-qPCR results for miR and gene expression changes are summarized below and in Tables 1-10.

- 1) In the 24 h RIHD model, 1 miR (rno-miR-672-5p) and 42 genes were up-regulated, and 2 miRs (rno-miR-142-5p and rno-miR-363-5p) and 16 genes were downregulated compared to the control group (see Tables 1-2 for genes).
- 2) In the 1-week RIHD model, 7 miRs (rno-miR-200b-3p, rno-miR-383-5p, rno-miR-471-5p, rno-miR-743a-3p, rno-miR-743b-3p, rno-miR-871-3p, rno-miR-1298) and 24 genes were up-regulated, and 5 miRs (rno-miR-34b-3p, rno-miR-34b-5p, rno-miR-34c-3p, rno-miR-34c-5p, rno-miR-322-3p) and 6 genes were downregulated compared to the control group. Additionally, LV expression of 2 miRs (rno-miR-208b-3p and rno-miR-672-5p) showed an increasing tendency in the RT group compared to the control group (see Table 3 for genes).
- 3) In the 3-week RIHD model, 7 miRs (rno-miR-9b-5p, rno-miR-21-5p, rno-miR-34a-5p, rno-miR-383-5p, miR-672-5p, rno-miR-743a-5p, rno-miR-1298) and 25 genes up-regulated, and 1 miR (rno-miR-322-5p) and 2 genes were down-regulated compared to the control group. Additionally, LV expression of 4 miRs (rno-miR-190b-5p, rno-miR-223-3p, rno-miR-741-3p, rno-miR-7578) showed an increasing tendency in the RT group compared to the control group (see Table 4 for genes).
- 4) In the 15-week RIHD model, 12 miRs and 6 genes were up-regulated, and 28 miRs and 16 genes were down-regulated compared to the control group (see Table 5 for miRs and Table 6 for genes)
- 5) In the 19-week RIHD model, 40 miRs and 79 genes were up-regulated, and 23 miRs and 45 genes were down-regulated compared to the control group (see Tables 7-8 for miRs and Tables 9-10 for genes).
- 6) The LV expression changes of selected miRs were also validated by RT-qPCR at several FUP time points. In pressure-overload-induced heart failure, the miR-212-3p/132-3p cluster is a crucial regulator of pathologic LVH via FOXO3-mediated pathways. In our experiments, at weeks 3 and 19, the RT-induced LV overexpression of the miR-212-3p was validated, and the expression of its selected target genes, including *Foxo3*, was also investigated by RT-qPCR (Sárközy M *et al.*, Front. Oncol., 2019, <https://doi.org/10.3389/fonc.2019.00598>). In contrast to the repression of *Foxo3* in the RT group at week 19, the total FOXO3 protein level failed to decrease in response to heart irradiation. Other selected hypertrophy-associated target genes of

miR-212-3p failed to change at the mRNA level in RIHD at week 19. In the 3<sup>rd</sup> and 19<sup>th</sup> FUP week, LVH was associated with the LV overexpression of miR-212-3p in our RIHD models. Therefore, miR-212-3p seems to play a role in the development of LVH via FOXO3-independent mechanisms in RIHD (Sárközy M *et al.*, Front Oncol, 2019, <https://doi.org/10.3389/fonc.2019.00598>).

- 7) Based on the NGS data, in our 19-week RIHD model, we found 51 miR-mRNA target pairs with opposite expression changes that are associated with cardiac hypertrophy or fibrosis according to databases and literature data (*e.g.*, up-regulation of miR-34a-5p and down-regulation of decorin; up-regulation of miR-132-3p and down-regulation of Wilms tumor-1 gene; or downregulation of miR-9a-5p and upregulation of tenascin-C; down-regulation of miR-199-3p and up-regulation of fibronectin-1; down-regulation of miR-9a-5p and up-regulation of neural cell adhesion molecule-1). The RT-induced LV up-regulation of tenascin-C was already validated by RT-qPCR; further RT-qPCR measurements are in progress.
- 8) In the 3-week FUP-time RIHD model, the up-regulation of the pro-fibrotic miR-21-5p, the pro-senescent miR-34a-5p, and the pro-atherosclerotic and the pro-inflammatory miR-223-5p were validated by RT-qPCR. Moreover, these miRs were significantly up-regulated in the 1-week FUP time RIHD model measured by RT-qPCR. However, at week 15, the expression of the pro-fibrotic miR-21-5p and miR-743a-3p were unchanged, and miR-741-3p, miR-881-3p, and miR-1298 were undetectable by RT-qPCR. In contrast to the NGS results, in the 15-week FUP time RIHD model, the pro-inflammatory miR-223-3p and the oxidative-stress associated miR-383-5p were significantly up-regulated, and the pro-senescent miR-34a and the pro-fibrotic and angiogenetic miR-130a-5p were significantly downregulated as compared to the control group by RT-qPCR.
- 9) In the 3- and 19-week RIHD models, 5 miRs [(miR-34a-5p, miR-383-5p, miR-741-3p, miR-743a-5p, and miR-881-3p (the latter two miR showed increasing tendency at week 3))] were up-regulated by NGS, and no down-regulated miR was shared between these two follow-up time points.
- 10) Several genes showed significant LV overexpression 24 h, 1, and 3 weeks after RT, including matrix metalloprotease-2 (*Mmp2*), apoptosis enhancing nuclease (*Aen*), growth differentiation factor 15 (*Gdf15*), epoxide hydrolase 1 (*Ephx1*), and Cd80 molecule (*Cd80*). Other genes, including G-2 and S-phase expressed 1 (*Gtse*) and glycoprotein nmb (*Gpnmb*), were significantly overexpressed 24 h, 1, 3, and 19 weeks after RT. Interestingly, leukocyte receptor tyrosine kinase (*Ltk*) was significantly overexpressed 24 h, 3, and 19 weeks after RT. In contrast, perforin (*Per*), killer cell lectin-like receptor D1 (*Klrd1*), and CD96 molecule (*Cd96*) were significantly downregulated 24 h and 19 weeks after RT.
- 11) We had technical difficulties comparing NGS results for miRs in blood plasma and LV tissue samples due to the low or undetectable levels of several miRs in the plasma samples. In the EDTA plasma samples (2 mL/animal), there were a lot of fragment mRNAs and other reads (even with >20 million read counts). After filtering, the 22 nt miRs had fewer and very different read counts (20 000-700 000). Therefore, the bioinformatics analysis might lead to false results. Due to the dubious results of the plasma NGS analysis, we preferred to perform proteomics measurements (it was not a commitment of the original project plan) from our LV tissue samples (n=6 in each group in each FUP time) to strengthen our NGS data for gene expression changes.
- 12) In the 24-h FUP time RT group, there were rather tendencies but no significant changes in the proteome compared to the control group in our hands. In the later FUP time points (*i.e.*, 1, 3, 15, and 19 weeks), 218 proteins showed significant expressional changes. Based on cluster analysis, 26 proteins responsible for fatty acid and lipid synthesis and 3 proteins involved in the regulation of cholesterol synthesis and homeostasis were repressed 3, 15, and 19 weeks after RT. In another cluster, 24 proteins associated with the structure of the heart, and 9 proteins involved in cardiac development and assembly of the myofibrils were overexpressed from week 3 in consonance with the LVH development assessed by echocardiography in the RT groups. Moreover, 6

proteins regulating the immune response or involved in the formation of antigens and immunoglobulins increased significantly 1 and 3 weeks after RT, corresponding with the inflammatory gene expressional changes assessed by RT-qPCR. 5 proteins involved in hemoglobin synthesis or the regulation of oxygen transport were overexpressed at weeks 3 and 19, probably as a compensatory mechanism to anemia and LV hypoxia due to LVH and fibrosis in the RT groups. Interestingly, the proteins forming the mitochondrial respiratory chain complex I were overexpressed at week 1 and were the most abundant in this cluster. Complex I is thought to be a key component in cardiomyopathy and is also important for the generation of reactive oxygen species. 31 of the 47 proteins forming complex I were found in this cluster, indicating a significant change. Importantly, several proteins involved in collagen synthesis were up-regulated 19 weeks after RT in accordance with the histology results. Unfortunately, we cannot discuss all of the proteins showing significant expression change in details due to the 25-page limitation of this final report.

- 13) Interestingly, 5 genes, *i.e.*, elastin microfibril interfacer 1 (*Emilin1*); apolipoprotein E (*ApoE*); S100 calcium-binding protein A4 (*S100a4*); and lumican (*Lum*); capping actin protein, gelsolin like (*Capg*) showed significant overexpression both at the mRNA and the protein levels in response to RT. *Emilin1*, *ApoE*, and *S100a4* were overexpressed 19 weeks, *Lum* 15 weeks, and *Capg* 1 week after RT in the LV tissue samples.
- 14) Due to the plethora of NGS and proteomics data and the few similarities in the LV gene expression changes at the mRNA and the protein levels, we decided to publish our results in more manuscripts (*i.e.*, miR and mRNA expression changes separately from the proteomics results) involving Dr. Merse Kis, Dr. Klaudia Kupecz, Dr. Réka Losonczy, and Dr. Dávid Volford current PhD students to the literature search and article writing.

**Table 1:** Significantly down-regulated genes in the LV samples 24 h after RT

| ID                 | Gene Symbol           | Description  | Fold change | adj. P-value |
|--------------------|-----------------------|--|-------------|--------------|
| ENSRNOG00000023030 | <i>Cd96</i>           | CD96 molecule  | -39.76      | 0.002        |
| ENSRNOG00000060246 | <i>Klrd1</i>          | killer cell lectin-like receptor D1                        | -20.89      | 0.006        |
| ENSRNOG00000055197 | <i>AABR07027872.1</i> | NA   | -18.28      | 0.003        |
| ENSRNOG00000047414 | <i>AABR07058479.1</i> | NA   | -17.81      | 0.034        |
| ENSRNOG00000018458 | <i>Ncr1</i>           | natural cytotoxicity triggering receptor 1                 | -15.24      | 0.045        |
| ENSRNOG00000022110 | <i>Gcsam</i>          | germinal center-associated, signaling and motility         | -13.59      | 0.002        |
| ENSRNOG00000024428 | <i>Kif20a</i>         | kinesin family member 20A                                  | -9.92       | 0.034        |
| ENSRNOG00000002659 | <i>Ciita</i>          | class II, major histocompatibility complex, transactivator | -9.04       | 0.002        |
| ENSRNOG00000000562 | <i>Prfl</i>           | perforin 1   | -8.22       | 0.048        |
| ENSRNOG00000007310 | <i>Klrb1a</i>         | killer cell lectin-like receptor subfamily B, member 1A    | -7.30       | 0.038        |
| ENSRNOG00000048636 | <i>Il2rb</i>          | interleukin 2 receptor subunit beta                        | -6.57       | 0.002        |
| ENSRNOG00000000451 | <i>RT1-Ba</i>         | RT1 class II, locus Ba                                     | -4.81       | 0.003        |
| ENSRNOG00000032844 | <i>RT1-Da</i>         | RT1 class II, locus Da                                     | -4.60       | 0.002        |
| ENSRNOG00000033215 | <i>RT1-Db1</i>        | RT1 class II, locus Db1                                    | -4.38       | 0.026        |
| ENSRNOG00000038574 | <i>Rassf9</i>         | Ras association domain family member 9                     | -4.25       | 0.034        |
| ENSRNOG00000001005 | <i>Fcer2</i>          | Fc fragment of IgE receptor II                             | -4.00       | 0.009        |

**Table 2:** Significantly up-regulated genes in the LV samples 24 h after RT

| <b>ID</b>           | <b>Gene Symbol</b> | <b>Description</b>  | <b>Fold Change</b> | <b>adj. P-value</b> |
|---------------------|--------------------|---|--------------------|---------------------|
| ENSRNOG00000018198  | <i>Dapk1</i>       | death associated protein kinase 1   | 2.23               | 0.031               |
| ENSRNOG00000013668  | <i>Capg</i>        | capping actin protein. gelsolin like  | 2.31               | 0.021               |
| ENSRNOG00000011971  | <i>C1s</i>         | complement C1s  | 2.53               | 0.041               |
| ENSRNOG00000006304  | <i>Mdm2</i>        | MDM2 proto-oncogene   | 2.57               | 0.000               |
| ENSRNOG000000020876 | <i>Bax</i>         | BCL2 associated X. apoptosis regulator  | 2.72               | 0.025               |
| ENSRNOG000000037225 | <i>Tyms</i>        | thymidylate synthetase  | 2.91               | 0.019               |
| ENSRNOG00000008816  | <i>Gpnmb</i>       | glycoprotein nmb  | 3.00               | 0.041               |
| ENSRNOG00000018233  | <i>Gas6</i>        | growth arrest specific 6  | 3.02               | 0.000               |
| ENSRNOG000000037080 | <i>Adamts17</i>    | ADAM metalloproteinase with thrombospondin type 1 motif. 17                   | 3.24               | 0.039               |
| ENSRNOG00000007946  | <i>Bcl2l1</i>      | Bcl2-like 1   | 3.30               | 0.004               |
| ENSRNOG000000050473 | <i>Rps27l</i>      | ribosomal protein S27-like  | 3.30               | 0.000               |
| ENSRNOG000000026902 | <i>Lyve1</i>       | lymphatic vessel endothelial hyaluronan receptor 1                            | 3.45               | 0.000               |
| ENSRNOG000000032150 | <i>Adcy2</i>       | adenylate cyclase 2   | 3.66               | 0.049               |
| ENSRNOG00000009068  | <i>Phlda3</i>      | pleckstrin homology-like domain. family A. member 3                           | 3.69               | 0.000               |
| ENSRNOG00000017819  | <i>Cd14</i>        | CD14 molecule   | 3.98               | 0.019               |
| ENSRNOG00000008012  | <i>Abcb1a</i>      | ATP binding cassette subfamily B member 1A                                    | 3.98               | 0.000               |
| ENSRNOG00000005302  | <i>Slc2a9</i>      | solute carrier family 2 member 9  | 4.54               | 0.001               |
| ENSRNOG00000016695  | <i>Mmp2</i>        | matrix metalloproteinase 2  | 4.57               | 0.000               |
| ENSRNOG000000021669 | <i>Mybl1</i>       | myeloblastosis oncogene-like 1  | 4.58               | 0.004               |
| ENSRNOG00000015445  | <i>Mal</i>         | mal. T-cell differentiation protein   | 4.59               | 0.039               |
| ENSRNOG00000013484  | <i>Gsta1</i>       | glutathione S-transferase alpha 1   | 5.12               | 0.000               |
| ENSRNOG000000020579 | <i>Col7a1</i>      | collagen type VII alpha 1 chain   | 5.51               | 0.001               |
| ENSRNOG000000022710 | <i>Prrg4</i>       | proline rich and Gla domain 4   | 5.97               | 0.002               |
| ENSRNOG00000018421  | <i>Aen</i>         | apoptosis enhancing nuclease  | 6.25               | 0.000               |
| ENSRNOG00000007964  | <i>Tp53inp1</i>    | tumor protein p53 inducible nuclear protein 1                                 | 6.27               | 0.000               |
| ENSRNOG00000003515  | <i>Ephx1</i>       | epoxide hydrolase 1   | 8.08               | 0.000               |
| ENSRNOG00000016148  | <i>Gtse1</i>       | G-2 and S-phase expressed 1   | 8.32               | 0.000               |
| ENSRNOG00000002831  | <i>Wfikkn2</i>     | WAP. follistatin/kazal. immunoglobulin. kunitz and netrin domain containing 2 | 9.68               | 0.000               |
| ENSRNOG00000013018  | <i>Eda2r</i>       | ectodysplasin A2 receptor   | 9.80               | 0.001               |
| ENSRNOG00000005348  | <i>Pamr1</i>       | peptidase domain containing associated with muscle regeneration 1             | 11.46              | 0.000               |
| ENSRNOG000000029478 | <i>Cyp4f39</i>     | cytochrome P450. family 4. subfamily f. polypeptide 39                        | 12.67              | 0.017               |
| ENSRNOG00000000521  | <i>Cdkn1a</i>      | cyclin-dependent kinase inhibitor 1A  | 12.92              | 0.000               |
| ENSRNOG00000015421  | <i>Slc27a3</i>     | solute carrier family 27 member 3   | 13.75              | 0.001               |
| ENSRNOG00000001527  | <i>Cd80</i>        | Cd80 molecule   | 14.39              | 0.001               |
| ENSRNOG000000025130 | <i>Ltk</i>         | leukocyte receptor tyrosine kinase  | 15.99              | 0.009               |
| ENSRNOG00000000500  | <i>Scube3</i>      | signal peptide. CUB domain and EGF like domain containing 3                   | 16.11              | 0.045               |
| ENSRNOG000000020552 | <i>Fosl1</i>       | FOS like 1. AP-1 transcription factor subunit                                 | 20.75              | 0.026               |
| ENSRNOG000000026870 | <i>Clic6</i>       | chloride intracellular channel 6  | 30.52              | 0.045               |
| ENSRNOG00000019661  | <i>Gdf15</i>       | growth differentiation factor 15  | 43.06              | 0.003               |

|                    |              |  |       |       |
|--------------------|--------------|--|-------|-------|
| ENSRNOG00000006471 | <i>Pvalb</i> | parvalbumin                                    | 55.09 | 0.001 |
| ENSRNOG00000005277 | <i>Ptpv</i>  | protein tyrosine phosphatase, receptor type, V | 60.13 | 0.000 |

**Table 3:** Significantly down- and up-regulated genes in the LV samples 1 week after RT

| ID                  | Gene Symbol           | Description   | Fold change | adj. P-value |
|---------------------|-----------------------|---|-------------|--------------|
| ENSRNOG000000020563 | <i>Cma1</i>           | chymase 1   | -21.14      | 0.020        |
| ENSRNOG000000014448 | <i>Arntl</i>          | aryl hydrocarbon receptor nuclear translocator-like                           | -5.57       | 0.007        |
| ENSRNOG000000015071 | <i>Zim1</i>           | zinc finger, imprinted 1  | -5.20       | 0.011        |
| ENSRNOG000000022110 | <i>Gcsam</i>          | germinal center-associated, signaling and motility                            | -4.21       | 0.043        |
| ENSRNOG000000013408 | <i>Npas2</i>          | neuronal PAS domain protein 2   | -3.65       | 0.003        |
| ENSRNOG000000000885 | <i>Auts2</i>          | autism susceptibility candidate 2   | -2.51       | 0.033        |
| ENSRNOG000000042785 | <i>Sesn2</i>          | sestrin 2   | 2.35        | 0.032        |
| ENSRNOG000000060511 | <i>Tcap</i>           | titin-cap   | 2.44        | 0.019        |
| ENSRNOG000000008012 | <i>Abcb1a</i>         | ATP binding cassette subfamily B member 1A                                    | 2.47        | 0.002        |
| ENSRNOG000000016695 | <i>Mmp2</i>           | matrix metalloproteinase 2  | 2.73        | 0.000        |
| ENSRNOG000000007964 | <i>Tp53inp1</i>       | tumor protein p53 inducible nuclear protein 1                                 | 2.77        | 0.001        |
| ENSRNOG000000050473 | <i>Rps27l</i>         | ribosomal protein S27-like  | 2.81        | 0.000        |
| ENSRNOG000000013484 | <i>Gstal</i>          | glutathione S-transferase alpha 1   | 2.93        | 0.007        |
| ENSRNOG000000008816 | <i>Gpnmb</i>          | glycoprotein nmb  | 2.97        | 0.017        |
| ENSRNOG000000009068 | <i>Phlda3</i>         | pleckstrin homology-like domain, family A, member 3                           | 3.71        | 0.000        |
| ENSRNOG000000018421 | <i>Aen</i>            | apoptosis enhancing nuclease  | 4.02        | 0.000        |
| ENSRNOG000000016945 | <i>Pla2g2a</i>        | phospholipase A2 group IIA  | 4.63        | 0.042        |
| ENSRNOG000000018413 | <i>Per3</i>           | period circadian clock 3  | 5.17        | 0.003        |
| ENSRNOG000000016148 | <i>Gtse1</i>          | G-2 and S-phase expressed 1   | 6.16        | 0.003        |
| ENSRNOG000000028247 | <i>Ankrd13d</i>       | ankyrin repeat domain 13D   | 6.52        | 0.020        |
| ENSRNOG000000013018 | <i>Eda2r</i>          | ectodysplasin A2 receptor   | 6.79        | 0.009        |
| ENSRNOG000000021027 | <i>Dbp</i>            | D-box binding PAR bZIP transcription factor                                   | 7.23        | 0.011        |
| ENSRNOG000000003515 | <i>Ephx1</i>          | epoxide hydrolase 1   | 9.06        | 0.000        |
| ENSRNOG000000002831 | <i>Wfikkn2</i>        | WAP, follistatin/kazal, immunoglobulin, kunitz and netrin domain containing 2 | 9.71        | 0.001        |
| ENSRNOG000000054768 | <i>AABR07050487.1</i> | NA  | 16.04       | 0.023        |
| ENSRNOG000000001527 | <i>Cd80</i>           | Cd80 molecule   | 16.34       | 0.005        |
| ENSRNOG000000019661 | <i>Gdf15</i>          | growth differentiation factor 15  | 41.05       | 0.024        |
| ENSRNOG000000005277 | <i>Ptpv</i>           | protein tyrosine phosphatase, receptor type, V                                | 48.99       | 0.000        |

**Table 4:** Significantly down- and up-regulated genes in the LV samples 3 weeks after RT

| <b>ID</b>           | <b>Gene Symbol</b> | <b>Description</b>                                       | <b>Fold Change</b> | <b>adj. P-value</b> |
|---------------------|--------------------|--|--------------------|---------------------|
| ENSRNOG00000002916  | <i>Car4</i>        | carbonic anhydrase 4                                     | -4.43              | 0.021               |
| ENSRNOG000000027730 | <i>Nxpe1</i>       | neurexophilin and PC-esterase domain family, member 1    | -2.35              | 0.002               |
| ENSRNOG000000016695 | <i>Mmp2</i>        | matrix metalloproteinase 2                               | 2.01               | 0.000               |
| ENSRNOG000000018414 | <i>Csf1r</i>       | colony stimulating factor 1 receptor                     | 2.15               | 0.049               |
| ENSRNOG000000012807 | <i>C1qa</i>        | complement C1q A chain                                   | 2.23               | 0.017               |
| ENSRNOG000000050697 | <i>Ctsz</i>        | cathepsin Z  | 2.39               | 0.033               |
| ENSRNOG000000009068 | <i>Phlda3</i>      | pleckstrin homology-like domain, family A, member 3      | 2.68               | 0.007               |
| ENSRNOG000000016038 | <i>Mgmt</i>        | O-6-methylguanine-DNA methyltransferase                  | 2.82               | 0.038               |
| ENSRNOG000000020918 | <i>Ccnd1</i>       | cyclin D1  | 2.90               | 0.000               |
| ENSRNOG000000008816 | <i>Gpnmb</i>       | glycoprotein nmb   | 2.93               | 0.017               |
| ENSRNOG000000018421 | <i>Aen</i>         | apoptosis enhancing nuclease                             | 3.24               | 0.000               |
| ENSRNOG000000003984 | <i>Apln</i>        | apelin   | 3.27               | 0.000               |
| ENSRNOG000000019728 | <i>Itgad</i>       | integrin subunit alpha D                                 | 3.28               | 0.007               |
| ENSRNOG000000019270 | <i>P2ry6</i>       | pyrimidinergic receptor P2Y6                             | 3.76               | 0.018               |
| ENSRNOG000000000187 | <i>Csf2rb</i>      | colony stimulating factor 2 receptor beta common subunit | 3.84               | 0.021               |
| ENSRNOG000000010018 | <i>Clec4a3</i>     | C-type lectin domain family 4, member A3                 | 4.00               | 0.013               |
| ENSRNOG000000000521 | <i>Cdkn1a</i>      | cyclin-dependent kinase inhibitor 1A                     | 5.10               | 0.000               |
| ENSRNOG000000048273 | <i>Apod</i>        | apolipoprotein D   | 10.18              | 0.047               |
| ENSRNOG000000025130 | <i>Ltk</i>         | leukocyte receptor tyrosine kinase                       | 10.34              | 0.042               |
| ENSRNOG000000013018 | <i>Eda2r</i>       | ectodysplasin A2 receptor                                | 12.51              | 0.021               |
| ENSRNOG000000012892 | <i>Abca4</i>       | ATP binding cassette subfamily A member 4                | 18.65              | 0.030               |
| ENSRNOG000000016148 | <i>Gtse1</i>       | G-2 and S-phase expressed 1                              | 19.18              | 0.000               |
| ENSRNOG000000001527 | <i>Cd80</i>        | Cd80 molecule  | 19.94              | 0.018               |
| ENSRNOG000000005277 | <i>Ptprv</i>       | protein tyrosine phosphatase, receptor type, V           | 22.37              | 0.000               |
| ENSRNOG000000048402 | <i>Igh-6</i>       | immunoglobulin heavy chain 6                             | 31.23              | 0.017               |
| ENSRNOG000000019661 | <i>Gdf15</i>       | growth differentiation factor 15                         | 78.56              | 0.013               |

**Table 5** Significantly down- and up-regulated miRs in the LV samples 15 weeks after RT

| <b>miR ID</b>          | <b>log fold change</b> | <b>adjusted p-value</b> |
|------------------------|------------------------|-------------------------|
| rno-miR-871-3p         | -6.18                  | 0.001                   |
| rno-miR-3064-3p        | -5.42                  | 0.001                   |
| rno-miR-124-5p         | -4.64                  | 0.034                   |
| rno-miR-144-3p         | -4.37                  | 0.009                   |
| rno-miR-743b-3p        | -4.30                  | 0.007                   |
| rno-miR-205            | -4.04                  | 0.015                   |
| rno-miR-743b-5p        | -3.94                  | 0.020                   |
| rno-miR-429            | -3.82                  | 0.036                   |
| rno-miR-200a-3p        | -3.73                  | 0.001                   |
| rno-miR-10b-5p         | -3.63                  | 0.018                   |
| rno-miR-451-5p         | -3.34                  | 0.000                   |
| rno-miR-743a-3p        | -3.10                  | 0.018                   |
| rno-miR-196b-5p        | -2.98                  | 0.004                   |
| rno-miR-881-3p         | -2.96                  | 0.035                   |
| rno-miR-10b-3p         | -2.93                  | 0.000                   |
| rno-miR-296-3p         | -2.74                  | 0.000                   |
| rno-miR-3064-5p        | -2.06                  | 0.007                   |
| rno-miR-490-5p         | -2.01                  | 0.000                   |
| rno-miR-34c-5p         | -2.00                  | 0.000                   |
| rno-miR-1949           | -1.98                  | 0.045                   |
| rno-miR-132-3p         | -1.89                  | 0.000                   |
| rno-miR-216b-5p        | -1.84                  | 0.014                   |
| rno-miR-223-5p         | -1.74                  | 0.007                   |
| rno-miR-511-3p         | -1.50                  | 0.041                   |
| rno-miR-34b-3p         | -1.48                  | 0.004                   |
| rno-miR-132-5p         | -1.44                  | 0.016                   |
| rno-miR-223-3p         | -1.15                  | 0.030                   |
| rno-miR-182            | -1.07                  | 0.024                   |
| <i>rno-miR-208a-3p</i> | <i>0.94</i>            | <i>0.016</i>            |
| <i>rno-miR-450b-5p</i> | <i>0.95</i>            | <i>0.001</i>            |
| rno-miR-181c-5p        | 1.07                   | 0.024                   |

|                 |      |       |
|-----------------|------|-------|
| rno-miR-195-5p  | 1.09 | 0.000 |
| rno-miR-450b-3p | 1.13 | 0.009 |
| rno-miR-127-3p  | 1.13 | 0.001 |
| rno-miR-150-3p  | 1.15 | 0.005 |
| rno-miR-503-5p  | 1.15 | 0.002 |
| rno-miR-363-3p  | 1.21 | 0.014 |
| rno-miR-325-5p  | 1.56 | 0.016 |
| rno-miR-547-5p  | 1.69 | 0.003 |
| rno-miR-485-3p  | 1.89 | 0.049 |
| rno-miR-201-5p  | 2.00 | 0.000 |
| rno-miR-3585-3p | 2.10 | 0.000 |

**Table 6:** Significantly down- and up-regulated genes in the LV samples 15 weeks after RT

| ID                  | Gene Symbol       | Description  | Fold change | adj. P-value |
|---------------------|-------------------|--|-------------|--------------|
| ENSRNOG00000006579  | <i>Reg3g</i>      | regenerating family member 3 gamma                           | -87.15      | 0.037        |
| ENSRNOG00000010263  | <i>Cldn11</i>     | claudin 11   | -17.50      | 0.036        |
| ENSRNOG00000019763  | <i>Mlph</i>       | melanophilin   | -16.83      | 0.046        |
| ENSRNOG00000017539  | <i>Mmp9</i>       | matrix metalloproteinase 9                                   | -14.50      | 0.036        |
| ENSRNOG00000016583  | <i>RGD1561517</i> | similar to chromosome 20 open reading frame 144              | -11.71      | 0.045        |
| ENSRNOG00000020339  | <i>Neurl1</i>     | neuralized E3 ubiquitin protein ligase 1                     | -8.99       | 0.036        |
| ENSRNOG00000009599  | <i>Rwdd2a</i>     | RWD domain containing 2A                                     | -7.95       | 0.036        |
| ENSRNOG00000016696  | <i>Angpt2</i>     | angiopoietin 2   | -5.44       | 0.045        |
| ENSRNOG00000024349  | <i>Cbarp</i>      | CACN beta subunit associated regulatory protein              | -4.30       | 0.037        |
| ENSRNOG00000019296  | <i>Gnat2</i>      | G protein subunit alpha transducin 2                         | -4.16       | 0.047        |
| ENSRNOG00000000693  | <i>Svop</i>       | SV2 related protein  | -3.90       | 0.046        |
| ENSRNOG00000010199  | <i>Glrb</i>       | glycine receptor, beta                                       | -3.90       | 0.046        |
| ENSRNOG00000003984  | <i>Apln</i>       | apelin   | -3.81       | 0.046        |
| ENSRNOG00000022521  | <i>Ddias</i>      | DNA damage-induced apoptosis suppressor                      | -3.31       | 0.046        |
| ENSRNOG000000033893 | <i>Cacna1h</i>    | calcium voltage-gated channel subunit alpha H                | -2.32       | 0.036        |
| ENSRNOG00000021729  | <i>Iqub</i>       | IQ motif and ubiquitin domain containing                     | -2.09       | 0.048        |
| ENSRNOG00000049471  | <i>Steap3</i>     | STEAP3 metalloproteinase                                     | 2.08        | 0.048        |
| ENSRNOG00000010205  | <i>Mturn</i>      | maturin, neural progenitor differentiation regulator homolog | 2.17        | 0.046        |
| ENSRNOG00000022337  | <i>Slitrk6</i>    | SLIT and NTRK-like family, member 6                          | 2.99        | 0.046        |
| ENSRNOG00000017064  | <i>Tdrd1</i>      | tudor domain containing 1                                    | 3.01        | 0.036        |
| ENSRNOG00000001171  | <i>Coq5</i>       | coenzyme Q5, methyltransferase                               | 3.26        | 0.036        |
| ENSRNOG00000011022  | <i>Mep1a</i>      | meprin 1 subunit alpha                                       | 16.42       | 0.046        |

**Table 7** Significantly down-regulated miRs in the LV samples 19 weeks after RT

| <b>miR ID</b>   | <b>log fold change</b> | <b>adj. P-value</b> |
|-----------------|------------------------|---------------------|
| rno-miR-6321    | -4.538                 | 0.044               |
| rno-miR-1247-5p | -2.402                 | 0.027               |
| rno-miR-3585-5p | -2.206                 | 0.002               |
| rno-miR-201-5p  | -2.105                 | 0.001               |
| rno-miR-547-3p  | -1.959                 | 0.001               |
| rno-miR-3585-3p | -1.799                 | 0.002               |
| rno-miR-547-5p  | -1.679                 | 0.002               |
| rno-miR-509-3p  | -1.656                 | 0.018               |
| rno-miR-338-3p  | -1.573                 | 0.006               |
| rno-miR-363-3p  | -1.439                 | 0.003               |
| rno-miR-148a-3p | -1.399                 | 0.009               |
| rno-miR-224-5p  | -1.302                 | 0.048               |
| rno-miR-214-5p  | -1.298                 | 0.032               |
| rno-miR-148a-5p | -1.180                 | 0.031               |
| rno-miR-195-3p  | -1.102                 | 0.027               |
| rno-miR-338-5p  | -1.090                 | 0.049               |
| rno-miR-150-3p  | -1.062                 | 0.024               |
| rno-miR-204-5p  | -1.044                 | 0.028               |
| rno-miR-9a-5p   | -0.956                 | 0.022               |
| rno-miR-151-5p  | -0.879                 | 0.048               |
| rno-miR-199a-3p | -0.852                 | 0.032               |
| rno-miR-150-5p  | -0.705                 | 0.028               |

**Table 8** Significantly up-regulated miRs in the LV samples 19 weeks after RT

| <b>miR ID</b>   | <b>log fold change</b> | <b>adj. P-value</b> |
|-----------------|------------------------|---------------------|
| rno-miR-221-3p  | 1.028                  | 0.005               |
| rno-miR-3102    | 1.073                  | 0.027               |
| rno-miR-193a-5p | 1.074                  | 0.018               |
| rno-miR-409a-5p | 1.156                  | 0.058               |
| rno-miR-296-5p  | 1.162                  | 0.028               |
| rno-miR-223-3p  | 1.215                  | 0.004               |
| rno-miR-21-5p   | 1.234                  | 0.000               |
| rno-miR-132-5p  | 1.254                  | 0.058               |
| rno-miR-511-3p  | 1.329                  | 0.032               |
| rno-miR-298-3p  | 1.347                  | 0.023               |
| rno-miR-182     | 1.379                  | 0.001               |
| rno-miR-132-3p  | 1.406                  | 0.006               |
| rno-miR-34a-5p  | 1.434                  | 0.001               |
| rno-miR-466c-5p | 1.508                  | 0.024               |
| rno-miR-653-5p  | 1.565                  | 0.037               |

|                  |       |       |
|------------------|-------|-------|
| rno-miR-183-5p   | 1.586 | 0.005 |
| rno-miR-212-3p   | 1.778 | 0.074 |
| rno-miR-34c-3p   | 1.800 | 0.004 |
| rno-miR-212-5p   | 1.856 | 0.008 |
| rno-miR-34b-3p   | 1.982 | 0.000 |
| rno-miR-129-5p   | 1.999 | 0.000 |
| rno-miR-298-5p   | 2.055 | 0.000 |
| rno-miR-296-3p   | 2.078 | 0.002 |
| rno-miR-34b-5p   | 2.211 | 0.018 |
| rno-miR-34c-5p   | 2.348 | 0.000 |
| rno-miR-129-2-3p | 2.450 | 0.048 |
| rno-miR-10b-3p   | 2.587 | 0.002 |
| rno-miR-871-3p   | 2.593 | 0.032 |
| rno-miR-205      | 2.691 | 0.001 |
| rno-miR-9b-5p    | 2.764 | 0.019 |
| rno-miR-10b-5p   | 2.885 | 0.000 |
| rno-miR-383-5p   | 2.900 | 0.002 |
| rno-miR-881-3p   | 2.973 | 0.026 |
| rno-miR-743a-5p  | 2.984 | 0.001 |
| rno-miR-741-3p   | 3.017 | 0.009 |
| rno-miR-743a-3p  | 3.696 | 0.016 |
| rno-miR-743b-3p  | 3.919 | 0.004 |
| rno-miR-1298     | 4.589 | 0.000 |
| rno-miR-196b-5p  | 5.026 | 0.004 |

**Table 9** Significantly down-regulated genes in the LV samples 19 weeks after RT

| ID                 | Gene Symbol           | Description                                   | Fold change | adj. P-value |
|--------------------|-----------------------|---|-------------|--------------|
| ENSRNOG00000034290 | <i>Ccl21</i>          | C-C motif chemokine ligand 21                 | -25.74      | 0.035        |
| ENSRNOG00000005639 | <i>Ar</i>             | androgen receptor                             | -15.54      | 0.039        |
| ENSRNOG00000060246 | <i>Klrd1</i>          | killer cell lectin like receptor D1           | -12.44      | 0.004        |
| ENSRNOG00000057957 | <i>Aim1l</i>          | absent in melanoma 1-like                     | -12.35      | 0.035        |
| ENSRNOG00000024986 | <i>Mmr1</i>           | multimerin 1                                  | -11.88      | 0.048        |
| ENSRNOG00000051837 | <i>Nwd2</i>           | NACHT and WD repeat domain containing 2       | -11.41      | 0.048        |
| ENSRNOG00000023030 | <i>Cd96</i>           | CD96 molecule                                 | -10.31      | 0.048        |
| ENSRNOG00000030763 | <i>Dpp4</i>           | dipeptidylpeptidase 4                         | -10.06      | 0.001        |
| ENSRNOG00000003221 | <i>Myoc</i>           | myocilin                                      | -9.82       | 0.013        |
| ENSRNOG00000004712 | <i>Angptl1</i>        | angiopoietin-like 1                           | -7.97       | 0.000        |
| ENSRNOG00000019120 | <i>Hmgcs2</i>         | 3-hydroxy-3-methylglutaryl-CoA synthase 2     | -7.85       | 0.038        |
| ENSRNOG00000034191 | <i>Fmol</i>           | flavin containing monooxygenase 1             | -7.37       | 0.002        |
| ENSRNOG00000015519 | <i>Ces1d</i>          | carboxylesterase 1D                           | -7.20       | 0.001        |
| ENSRNOG00000002244 | <i>Pdgfra</i>         | platelet derived growth factor receptor alpha | -7.18       | 0.000        |
| ENSRNOG00000047307 | <i>Cntfr</i>          | ciliary neurotrophic factor receptor          | -7.07       | 0.002        |
| ENSRNOG00000055197 | <i>AABR07027872.1</i> | NA  | -6.67       | 0.013        |

|                     |                              |   |       |       |
|---------------------|------------------------------|---|-------|-------|
| ENSRNOG00000016136  | <i>Pdcd1lg2</i>              | programmed cell death 1 ligand 2  | -6.12 | 0.042 |
| ENSRNOG00000060130  | <i>Ypel4</i>                 | yippee-like 4   | -6.08 | 0.048 |
| ENSRNOG00000000562  | <i>Prfl</i>                  | perforin 1  | -6.00 | 0.041 |
| ENSRNOG00000018991  | <i>Gsn</i>                   | gelsolin  | -5.66 | 0.000 |
| ENSRNOG00000013074  | <i>Wtl</i>                   | Wilms tumor 1   | -4.98 | 0.014 |
| ENSRNOG00000033087  | <i>Cdh23</i>                 | cadherin-related 23   | -4.81 | 0.011 |
| ENSRNOG00000008182  | <i>Htra3</i>                 | HtrA serine peptidase 3   | -4.79 | 0.000 |
| ENSRNOG000000061379 | <i>C7</i>                    | complement C7   | -4.76 | 0.003 |
| ENSRNOG00000006119  | <i>Slc7a15</i>               | solute carrier family 7 (cationic amino acid transporter, y <sup>+</sup> system), member 15 | -4.69 | 0.032 |
| ENSRNOG000000057501 | <i>Fam81a</i>                | family with sequence similarity 81, member A  | -4.47 | 0.005 |
| ENSRNOG000000003510 | <i>Fmo2</i>                  | flavin containing monooxygenase 2   | -4.07 | 0.019 |
| ENSRNOG000000004147 | <i>Abca8a</i>                | ATP-binding cassette, subfamily A (ABC1), member 8a   | -3.87 | 0.002 |
| ENSRNOG000000021220 | <i>Cpxm1</i>                 | carboxypeptidase X (M14 family), member 1   | -3.60 | 0.009 |
| ENSRNOG000000013102 | <i>Entpd2</i>                | ectonucleoside triphosphate diphosphohydrolase 2  | -3.50 | 0.019 |
| ENSRNOG000000011548 | <i>Ebf2</i>                  | early B-cell factor 2   | -3.42 | 0.014 |
| ENSRNOG000000023008 | <i>Fam131c</i>               | family with sequence similarity 131, member C   | -3.39 | 0.041 |
| ENSRNOG000000014137 | <i>Fbln1</i>                 | fibulin 1   | -3.36 | 0.001 |
| ENSRNOG000000002947 | <i>Dpt</i>                   | dermatopontin   | -3.17 | 0.000 |
| ENSRNOG000000019518 | <i>Pde4c</i>                 | phosphodiesterase 4C  | -3.09 | 0.035 |
| ENSRNOG000000015318 | <i>Heyl</i>                  | hes-related family bHLH transcription factor with YRPW motif-like                           | -3.03 | 0.014 |
| ENSRNOG000000014232 | <i>P2ry1</i>                 | purinergic receptor P2Y1  | -3.02 | 0.042 |
| ENSRNOG000000019648 | <i>Col6a3</i>                | collagen type VI alpha 3 chain  | -2.95 | 0.009 |
| ENSRNOG000000055078 | <i>Cyp4b1</i>                | cytochrome P450, family 4, subfamily b, polypeptide 1                                       | -2.93 | 0.032 |
| ENSRNOG000000010529 | <i>Thbs2</i>                 | thrombospondin 2  | -2.77 | 0.034 |
| ENSRNOG000000004554 | <i>Dcn</i>                   | decorin   | -2.63 | 0.000 |
| ENSRNOG000000061768 | <i>Slc43a3</i>               | solute carrier family 43, member 3  | -2.57 | 0.021 |
| ENSRNOG000000029342 | <i>Scn7a</i>                 | sodium voltage-gated channel alpha subunit 7  | -2.51 | 0.035 |
| ENSRNOG000000009629 | <i>Car2</i>                  | carbonic anhydrase 2  | -2.50 | 0.047 |
| ENSRNOG000000004610 | <i>Lum</i>                   | lumican   | -2.45 | 0.042 |
| ENSRNOG000000014424 | <i>RGD</i><br><i>1563354</i> | similar to hypothetical protein D630003M21  | -2.41 | 0.035 |

**Table 10** Significantly down-regulated genes in the LV samples 19 weeks after RT

| ID                  | Gene Symbol                  | Description                                | Fold change | adj. P-value |
|---------------------|------------------------------|--|-------------|--------------|
| ENSRNOG00000008246  | <i>Emilin1</i>               | elastin microfibril interfacier 1          | 2.05        | 0.028        |
| ENSRNOG000000020918 | <i>Ccnd1</i>                 | cyclin D1                                  | 2.23        | 0.013        |
| ENSRNOG000000016343 | <i>Dkk3</i>                  | dickkopf WNT signaling pathway inhibitor 3 | 2.38        | 0.020        |
| ENSRNOG000000017431 | <i>RGD</i><br><i>1304884</i> | similar to RIKEN cDNA 6430548M08           | 2.54        | 0.035        |
| ENSRNOG000000012804 | <i>Clqc</i>                  | complement C1q C chain                     | 2.61        | 0.032        |
| ENSRNOG000000009019 | <i>Slc6a6</i>                | solute carrier family 6 member 6           | 2.62        | 0.048        |
| ENSRNOG000000012807 | <i>Clqa</i>                  | complement C1q A chain                     | 2.77        | 0.009        |
| ENSRNOG000000018454 | <i>ApoE</i>                  | apolipoprotein E                           | 2.89        | 0.006        |
| ENSRNOG000000017163 | <i>Pfkip</i>                 | phosphofructokinase, platelet              | 2.93        | 0.025        |

|                     |                  |  |       |       |
|---------------------|------------------|--|-------|-------|
| ENSRNOG0000000699   | <i>Selplg</i>    | selectin P ligand  | 3.05  | 0.020 |
| ENSRNOG00000003622  | <i>Cybb</i>      | cytochrome b-245 beta chain  | 3.09  | 0.020 |
| ENSRNOG000000028015 | <i>Pf4</i>       | platelet factor 4  | 3.10  | 0.021 |
| ENSRNOG000000009311 | <i>Fstl3</i>     | folliculin like 3  | 3.15  | 0.021 |
| ENSRNOG000000007415 | <i>Ptgs1</i>     | prostaglandin-endoperoxide synthase 1  | 3.16  | 0.030 |
| ENSRNOG000000003546 | <i>Tnfrsf12a</i> | TNF receptor superfamily member 12A  | 3.27  | 0.020 |
| ENSRNOG000000021669 | <i>Mybl1</i>     | myeloblastosis oncogene-like 1   | 3.41  | 0.050 |
| ENSRNOG000000001431 | <i>Rasa4</i>     | RAS p21 protein activator 4  | 3.43  | 0.025 |
| ENSRNOG000000007475 | <i>Gpihbp1</i>   | glycosylphosphatidylinositol anchored high density lipoprotein binding protein 1 | 3.43  | 0.006 |
| ENSRNOG000000057221 | <i>Scn3b</i>     | sodium voltage-gated channel beta subunit 3                                      | 3.57  | 0.041 |
| ENSRNOG000000005347 | <i>Fjx1</i>      | four jointed box 1   | 3.80  | 0.039 |
| ENSRNOG000000011821 | <i>S100a4</i>    | S100 calcium-binding protein A4  | 3.82  | 0.005 |
| ENSRNOG000000003772 | <i>Csrp2</i>     | cysteine and glycine-rich protein 2  | 3.84  | 0.032 |
| ENSRNOG000000005825 | <i>Lyz2</i>      | lysozyme 2   | 4.01  | 0.003 |
| ENSRNOG000000010208 | <i>Timp1</i>     | TIMP metalloproteinase inhibitor 1   | 4.02  | 0.008 |
| ENSRNOG000000001224 | <i>Itgb2</i>     | integrin subunit beta 2  | 4.08  | 0.014 |
| ENSRNOG000000016306 | <i>Adgrv1</i>    | adhesion G protein-coupled receptor V1   | 4.08  | 0.018 |
| ENSRNOG000000060237 | <i>Inhbb</i>     | inhibin beta B subunit   | 4.33  | 0.011 |
| ENSRNOG000000014117 | <i>Hmox1</i>     | heme oxygenase 1   | 4.34  | 0.010 |
| ENSRNOG000000019270 | <i>P2ry6</i>     | pyrimidinergic receptor P2Y6   | 4.51  | 0.021 |
| ENSRNOG000000017783 | <i>Sfrp1</i>     | secreted frizzled-related protein 1  | 4.56  | 0.000 |
| ENSRNOG000000031890 | <i>Ncam1</i>     | neural cell adhesion molecule 1  | 4.69  | 0.000 |
| ENSRNOG000000012229 | <i>Col18a1</i>   | collagen type XVIII alpha 1 chain  | 4.98  | 0.000 |
| ENSRNOG000000037632 | <i>LOC688553</i> | hypothetical protein LOC688553   | 4.99  | 0.028 |
| ENSRNOG000000010797 | <i>Esm1</i>      | endothelial cell-specific molecule 1   | 5.14  | 0.001 |
| ENSRNOG000000012660 | <i>Postn</i>     | periostin  | 5.18  | 0.029 |
| ENSRNOG000000014288 | <i>Fn1</i>       | fibronectin 1  | 5.26  | 0.001 |
| ENSRNOG000000038784 | <i>Piezo2</i>    | piezo-type mechanosensitive ion channel component 2                              | 5.52  | 0.032 |
| ENSRNOG000000043098 | <i>Mt2A</i>      | metallothionein 2A   | 5.59  | 0.009 |
| ENSRNOG000000054251 | <i>Clec7a</i>    | C-type lectin domain family 7, member A  | 5.61  | 0.034 |
| ENSRNOG000000012830 | <i>Paqr8</i>     | progesterone and adipoQ receptor family member 8                                 | 5.64  | 0.020 |
| ENSRNOG000000014361 | <i>Edn1</i>      | endothelin 1   | 5.68  | 0.003 |
| ENSRNOG000000001414 | <i>Serpine1</i>  | serpin family E member 1   | 5.74  | 0.014 |
| ENSRNOG000000009822 | <i>Tlr2</i>      | toll-like receptor 2   | 5.98  | 0.007 |
| ENSRNOG000000017676 | <i>Plvap</i>     | plasmalemma vesicle associated protein   | 6.32  | 0.004 |
| ENSRNOG000000008816 | <i>Gpnmb</i>     | glycoprotein nmb   | 6.50  | 0.000 |
| ENSRNOG000000016148 | <i>Gtse1</i>     | G-2 and S-phase expressed 1  | 7.07  | 0.019 |
| ENSRNOG000000016581 | <i>Serpib1a</i>  | serpin family B member 1A  | 7.29  | 0.011 |
| ENSRNOG000000047300 | <i>Bdkrb2</i>    | bradykinin receptor B2   | 7.30  | 0.002 |
| ENSRNOG000000017277 | <i>Igsf6</i>     | immunoglobulin superfamily, member 6   | 7.44  | 0.035 |
| ENSRNOG000000012094 | <i>Ltbp2</i>     | latent transforming growth factor beta binding protein 2                         | 7.96  | 0.041 |
| ENSRNOG000000018452 | <i>Unc13a</i>    | unc-13 homolog A   | 8.05  | 0.025 |
| ENSRNOG000000010516 | <i>Plau</i>      | plasminogen activator, urokinase   | 8.19  | 0.034 |
| ENSRNOG000000014653 | <i>Arl11</i>     | ADP-ribosylation factor like GTPase 11   | 8.26  | 0.002 |
| ENSRNOG000000038132 | <i>Vsig4</i>     | V-set and immunoglobulin domain containing 4                                     | 10.72 | 0.032 |
| ENSRNOG000000017054 | <i>Kcne3</i>     | potassium voltage-gated channel subfamily E regulatory subunit 3                 | 11.30 | 0.008 |
| ENSRNOG000000006735 | <i>Cdkn2b</i>    | cyclin-dependent kinase inhibitor 2B   | 11.49 | 0.028 |

|                     |                              |   |       |       |
|---------------------|------------------------------|---|-------|-------|
| ENSRNOG00000002343  | <i>Uchl1</i>                 | ubiquitin C-terminal hydrolase L1                         | 11.58 | 0.008 |
| ENSRNOG00000000700  | <i>Tmem119</i>               | transmembrane protein 119                                 | 12.21 | 0.009 |
| ENSRNOG000000056219 | <i>Olr1</i>                  | oxidized low density lipoprotein (lectin-like) receptor 1 | 12.39 | 0.006 |
| ENSRNOG000000027811 | <i>Lilrb4</i>                | leukocyte immunoglobulin like receptor B4                 | 13.47 | 0.001 |
| ENSRNOG000000017448 | <i>Exoc3l2</i>               | exocyst complex component 3-like 2                        | 13.68 | 0.049 |
| ENSRNOG000000020136 | <i>Tgml</i>                  | transglutaminase 1  | 13.93 | 0.017 |
| ENSRNOG000000027331 | <i>Ppefl</i>                 | protein phosphatase with EF-hand domain 1                 | 17.68 | 0.032 |
| ENSRNOG00000005277  | <i>Ptprv</i>                 | protein tyrosine phosphatase, receptor type, V            | 18.72 | 0.006 |
| ENSRNOG000000020552 | <i>Fosl1</i>                 | FOS like 1, AP-1 transcription factor subunit             | 19.68 | 0.018 |
| ENSRNOG000000036615 | <i>RGD</i><br><i>1560242</i> | similar to RIKEN cDNA 1700028P14                          | 20.89 | 0.009 |
| ENSRNOG000000025130 | <i>Ltk</i>                   | leukocyte receptor tyrosine kinase                        | 21.44 | 0.012 |
| ENSRNOG000000017625 | <i>Htr2b</i>                 | 5-hydroxytryptamine receptor 2B                           | 26.02 | 0.018 |
| ENSRNOG000000058645 | <i>Tnc</i>                   | tenascin C  | 27.36 | 0.000 |
| ENSRNOG000000006151 | <i>Reg3b</i>                 | regenerating family member 3 beta                         | 27.67 | 0.037 |
| ENSRNOG000000053766 | <i>Ramp3</i>                 | receptor activity modifying protein 3                     | 31.12 | 0.002 |
| ENSRNOG000000021796 | <i>RGD</i><br><i>1565166</i> | similar to MGC45438 protein                               | 32.73 | 0.004 |
| ENSRNOG000000023068 | <i>Cd5l</i>                  | Cd5 molecule-like   | 33.16 | 0.014 |
| ENSRNOG000000012892 | <i>Abca4</i>                 | ATP binding cassette subfamily A member 4                 | 34.61 | 0.001 |
| ENSRNOG000000016164 | <i>Fcrl2</i>                 | Fc receptor-like 2  | 53.45 | 0.014 |
| ENSRNOG000000030187 | <i>Mmp12</i>                 | matrix metalloproteinase 12                               | 77.61 | 0.001 |

#### 4.3. Experimental modification of RIHD with a new biological agent (Tasks 3)

The immunomodulatory, anti-apoptotic, and antioxidant effects of the preimplantation factor (PIF) were described in acute radiation syndrome and graft-versus-host disease. Therefore, we aimed to test the potential cardioprotective effects of PIF on the development of RIHD. Male Sprague-Dawley rats were divided into three groups: 1) control, 2) radiotherapy (RT, 50 Gy, delivered to the heart), 3) treated by PIF (*sc.* 1.5 mg/kg/day for 2 weeks then twice a week), and were followed for 1, 3, or 15 weeks. At the endpoints, cardiac function and morphology were assessed by echocardiography and histology, and left ventricular samples were collected for RT-qPCR and Western blot measurements.

At week 3, the PIF treatment markedly improved the echocardiographic parameters of diastolic dysfunction (*i.e.*,  $e'$  and  $E/e'$  ratio) and reduced the overexpression of the pro-inflammatory *Il1* and inflammation-associated inducible nitric oxide synthase (*Nos2*) compared to the RT-only group. At week 15, the RT-induced diastolic dysfunction was associated with significantly repressed sarcoendoplasmic reticulum ATPase 2a (SERCA2a) protein level and increased *Il6* expression. PIF ameliorated the RT-induced molecular changes at week 15. At week 3, PIF failed to ameliorate the mild LVH compared to the RT-only group. However, at week 15, PIF ameliorated the RT-induced severe concentric LVH (*i.e.*, reduced LV septal and inferior wall thicknesses and increased LV end-systolic and end-diastolic diameters) assessed by echocardiography (Figure 1), diminished the increased cardiomyocyte perimeters assessed on HE-stained slides, and reduced the hypertrophy and tissue hypoxia-associated *Myh7/Myh6* ratio as well as the cardiomyocyte stretch-associated A-type natriuretic peptide (*Nppa*). Moreover, PIF significantly reduced the RT-induced LV overexpression of the TGF- $\beta$  receptor at the protein level at week 3, and markedly decreased the LV overexpression of the connective tissue growth factor (*Ctgf*) and collagen-1a1 (*Coll1a1*), and the SMAD2/3 protein level in the canonical TGF-beta signaling pathway and decreased the pro-fibrotic and hypertrophic *Stat3* overexpression and the phospho-STAT3/STAT3 ratio at week 15. However, PIF failed to markedly reduce the interstitial fibrosis assessed on picrosirius red and fast green-stained slides, probably due to the high dose of RT (50 Gy). To decide if PIF has anti-fibrotic effects in our RIHD model, immunohistochemistry stainings for

COL1a1 and COL3a1 are in progress. Interestingly, the phospho-AKT/AKT, phospho-ERK1/ERK1, and phospho-ERK2/ERK2 ratios were significantly higher in response to PIF compared to the control or RT-only groups at week 3, probably indicating the activation of surviving gene program and maintaining the LVH development. (Indeed, PIF failed to reduce the mild LVH assessed by echocardiography at week 3). The over-activation of the tissue renin-angiotensin-aldosterone system (RAAS) is a well-known factor in LVH and fibrosis development in heart failure. The significant over-expression of the angiotensinogen (*Agt*) and the angiotensin-II type 1 receptor (*Agtr1*) were markedly reduced by PIF compared to the RT-only group at week 3. The alternative activators of the RAAS system, including chymase (*Cma1*) and plasminogen (*Pln*), showed an increasing tendency at week 3 and a significant increase in the RT-only group at week 15. The RT-induced overexpression of both genes was markedly reduced by PIF at week 15. Neuregulin-1 $\beta$  (*Nrg*) induced cardiomyocyte hypertrophy in several *in vivo* and *in vitro* models. In our present study, the LV expression of *Nrg* showed an increasing tendency at weeks 3 and 15 in the RT-only groups, and it was significantly ameliorated by PIF at week 15. The apoptosis marker BAX/BCL2 ratio was significantly higher in the RT groups independently of PIF treatment at weeks 1 and 3. The protein levels of apoptosis-inducing factor (AIF) and caspase-7 (CASP7) were not different between the groups at weeks 1 and 3. There were no significant differences in the measured apoptosis-associated proteins (BAX, BCL2, AIF, CASP7) between the groups at week 15. Moreover, we started new experiments in collaboration with Dr. Renáta Minorics and Prof. Dr. István Zupkó (Institute of Pharmacodynamics and Biopharmacy, University of Szeged, Hungary) beyond the original commitments of the present project to test the effects of PIF on 3 different types of breast cancer cell lines (MCF-7, T47D, MDA-MB-231) without or with irradiation (4 Gy) to enhance the translational value of our results. The PIF treatment did not influence the viability of unirradiated breast cancer cell lines. Importantly, PIF did not enhance cell proliferation in any breast cancer cell lines but increased the effectiveness of radiotherapy, particularly in the T47D cells (Figures 2-3). In conclusion, PIF reduced the severity of RIHD, probably via the inhibition of the TGF- $\beta$ /SMAD pathway. Since PIF did not enhance breast cancer cell proliferation, it could be an optimal candidate for the prevention of RIHD development in clinical trials. These results were shown at numerous national and international conferences during the project. The preparation of a manuscript summarizing the abovementioned results is in progress (our target journal is JACC: CardioOncology).

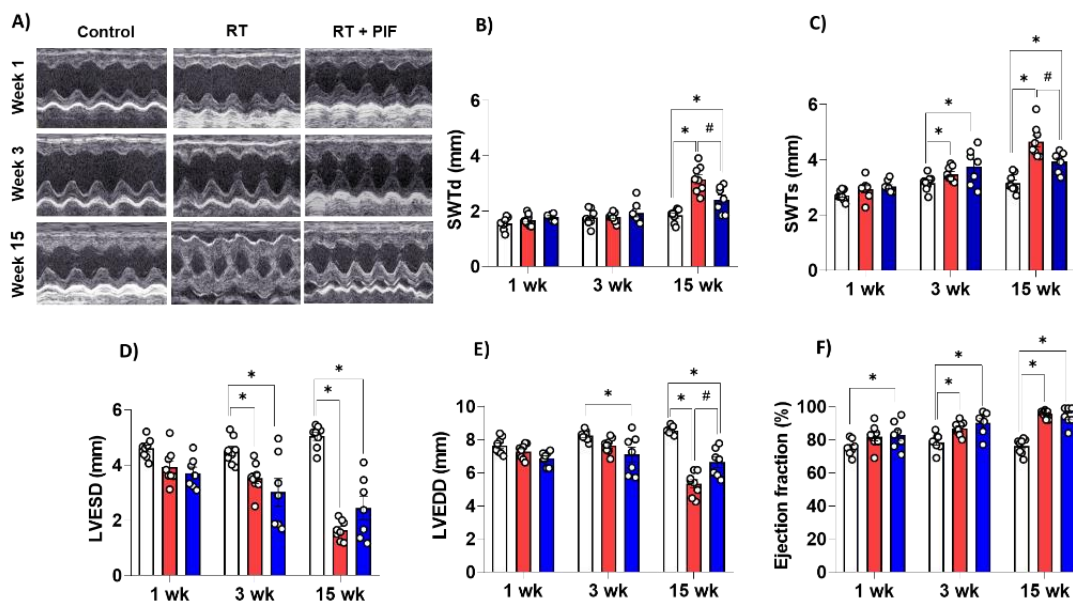


**Figure 1** PIF significantly ameliorated the severity of left ventricular hypertrophy in RIHD

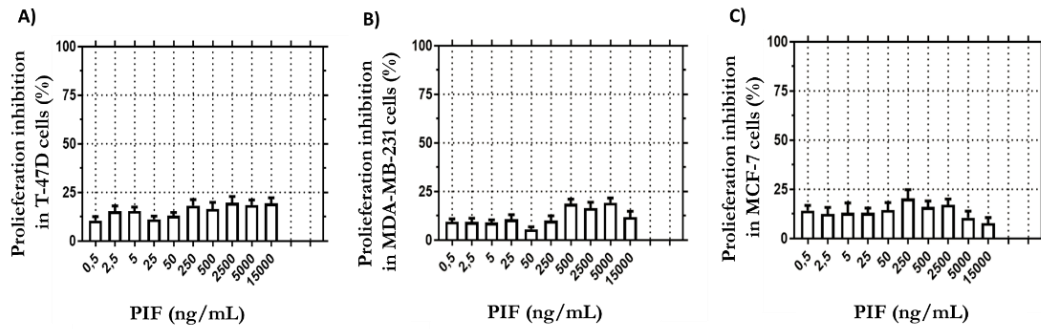


**Figure 2** The effect of PIF on cell division in human ductal and metastatic adenocarcinoma cell lines

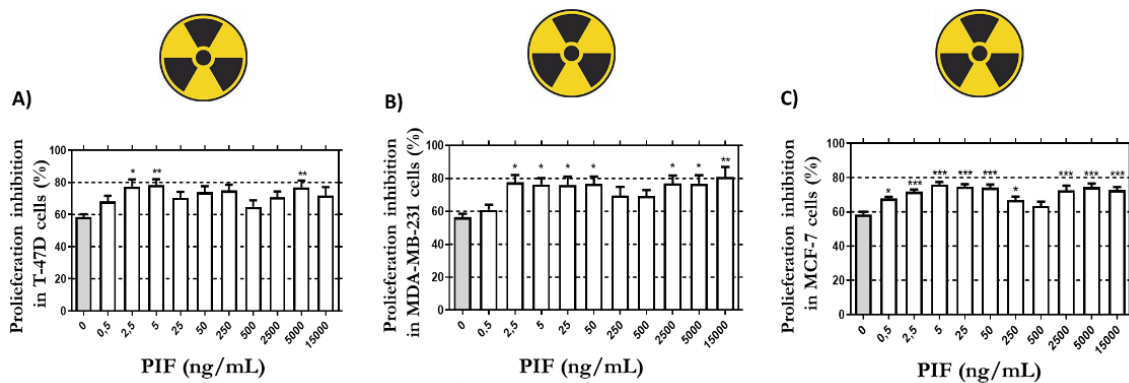


**Figure 3** PIF enhances the cell proliferation inhibitory effect of radiotherapy in human ductal and metastatic adenocarcinoma cell lines

Based on the RAAS gene expression results in the *in vivo* experiments with PIF in irradiated males, we aimed to investigate the effects of the angiotensin-II receptor blocker losartan (10 mg/kg/day) in our RIHD models beyond the original commitments of the present grant. At week 15 post-irradiation, losartan alleviated the echocardiographic and histological signs of LVH and fibrosis and reduced the LV overexpression of *Cmal*, *Ctgf*, and *Tgfb* measured by qPCR; likewise, it decreased the level of the SMAD2/3 protein determined by Western blot. In both RT groups, the pro-survival phospho-AKT/AKT and the phospho-ERK1/2/ERK1/2 ratios were increased at week 15. The anti-remodeling effects of losartan seem to be associated with the repression of chymase and several elements of the TGF- $\beta$ /SMAD signaling pathway in our RIHD model (Kovács MG *et al.*, Int. J Mol. Sci., 2021, doi: <https://doi.org/10.3390/ijms222312963>). In order to clarify whether losartan and other ARBs may be protective against RIHD in humans, clinical trials enrolling a large number of patients are required to widen the indication of this otherwise routinely used drug of heart failure treatment. Based on this publication, Dr. Mónika G. Kovács defended her Ph.D. thesis in 2022. Additionally, we investigated the effects of losartan with or without the  $\beta$ 3-adrenoceptor agonist mirabegron in another heart failure model (*i.e.*, uremic cardiomyopathy, Kovács ZZA *et al.*, Sci. Rep., 2021, <https://doi.org/10.1038/s41598-021-96815-5>.) and another onco-cardiologic model, (*i.e.*, doxorubicin-induced chronic cardiotoxicity, Freiwán *et al.*, Int. J Mol. Sci., 2022, doi: <https://doi.org/10.3390/ijms23042201>.) in two side projects. Based on these 2 publications, Dr. Zsuzsanna Kovács and Marah Freiwán defended their Ph.D. theses.

We also investigated the effects of PIF and losartan on selected miRs in the LV samples by RT-qPCR. The overexpression of the pro-fibrotic miR-21-5p was significantly decreased by PIF compared to the time-matched RT-only groups at weeks 1 and 3. The overexpression of the senescence-associated miR-34a-5p was significantly reduced by losartan compared to the RT-only group at week 3. The

overexpression of the miR-223-5p was tendentially decreased by losartan at week 3, and the overexpression of miR-383 was tendentially reduced by PIF at week 15. The repression of the miR-130a-5p was not influenced by PIF or losartan at any FUP time. There was no significant difference in the LV expression of miR-743a between the groups at week 15.

Moreover, we started new *in vivo* experiments to investigate the effects of PIF on RIHD development and behavior and stress axis in female Sprague-Dawley rats in collaboration with Dr. Krisztina Csabafi at the Department of Pathophysiology, Albert Szent-Györgyi Medical School, University of Szeged. However, we reduced the RT dose to 12 Gy in females to better mimic the real-life clinical scenario (*e.g.*, lower RT doses in breast cancer patients). Therefore, the development of RIHD was slower: LVH started to develop in the 6<sup>th</sup> FUP month assessed by echocardiography. We plan to terminate our experiment in the 9<sup>th</sup>-10<sup>th</sup> FUP months, depending on the echocardiographic results (this side project started in February 2023). We plan to measure similar endpoints by echocardiography, histology, RT-qPCR, and WB in females as in our male RIHD model detailed above. Moreover, we plan to perform additional behavior experiments and isolate the brain to investigate the effects of PIF on the relationship and molecular markers of heart failure and stress axis in RIHD.

#### ***4.4. Validation of the results of the acute in vivo experiments by PIF and/or miR-modulators in cell culture (Task 4)***

In non-irradiated H9c2 cardiomyoblasts, PIF did not influence cell viability tested in a broad concentration range (0.3-5000 ng/mL). During the *in vitro* radiation dose set-up experiments, the irradiation (1, 2, 5, and 10 Gy) of H9c2 cardiomyoblasts induced oxidative stress (superoxide anion formation), apoptotic cell death characterized by increased frequency of micronuclei formation, chromatin fragmentation, and condensation and reduced the cell viability in a dose-dependent manner. For further *in vitro* experiments, the highest irradiation dose (10 Gy) was chosen in H9c2 cardiomyoblasts. The effects of PIF (0.3-5000 ng/mL, 24 h treatment) were also tested in irradiated H9c2 cardiomyoblasts 48 hours post-irradiation. In the irradiated H9c2 cardiomyoblasts, PIF significantly reduced the cell death rate and oxidative stress in two distant concentrations (5 and 5000 ng/mL, n=7-14 and 7-28; 4 and 8 independent experiments, respectively). Therefore, in further *in vitro* experiments, PIF was used in these two concentrations. The irradiated (10 Gy) and PIF-treated (5 and 5000 ng/mL) H9c2 cardiomyoblast showed significantly fewer DNA double-strand breaks, apoptotic nuclei, cleaved/total-caspase-3 and cleaved/total-caspase 7 levels compared to the irradiated group (n=12-14, 2-4 independent experiments). However, there was no significant difference in the BAX, BCL-XL, phospho-STAT3/STAT3, and phospho-AKT/AKT ratios between the groups (n=9-11, 3 independent experiments).

Moreover, the effect of PIF (5 ng/mL) on the gene expression of the fibrosis markers *Coll1a1* and *Col3a1*, and the hypertrophy marker  $\alpha$ -smooth muscle actin (*Acta2*) was tested in TGF- $\beta$ -induced human ventricular cardiac fibroblasts (HVCFs) in collaboration with Dr. Attila Kiss, Dr. Péter Pokreisz, and Prof. Dr. Bruno K. Podesser, Ludwig Boltzmann Institute for Cardiovascular Research at Center for Biomedical Research and Translational Surgery, Medical University of Vienna, Vienna, Austria. In this low (*i.e.*, 5 ng/mL) concentration, PIF failed to reduce the expressions of *Coll1a1*, *Col3a1*, and *Acta2*. Further experiments with higher PIF concentrations are planned in HVCFs.

In conclusion, PIF showed direct anti-apoptotic and anti-oxidative effects in two distant concentrations in the *in vitro* cell culture experiments in the irradiated H9c2 cardiomyoblasts; however, it seems to exert its protective effects by activating different signaling pathways in the *in vitro* cell culture experiments compared to the *in vivo* RIHD models (see Task 3).

Beyond the original commitments of this project, the effects of PIF were also tested in another oxidative stress model, *i.e.*, acute doxorubicin-induced cardiotoxicity in H9c2 cardiomyoblasts pre-treated with PIF (0.3-5000 ng/mL) for 30 min or 24 h in a side experiment. PIF improved the cell viability and reduced the oxidative stress in more concentrations in the 24 h pre-treatment experiments. Finally, the 10 and 20 ng/mL PIF concentrations were chosen for further *in vitro* experiments. In

response to PIF, there were significantly fewer apoptotic nuclei, DNA double-strand breaks, and cleaved/total caspase-3 levels compared to the irradiated group (n=8-15, 2-3 independent experiments). However, there was no significant difference in the apoptosis-associated BAX, BCL-XL, and AIF levels between the groups (n=9-11, 3 independent experiments).

To strengthen the *in vivo* NGS results at miR and mRNA levels, RNA samples were prepared from non-irradiated and irradiated cells. For the transfection experiments, the optimal duration of transfection, concentration of miRs, and transfection reagents were optimized. However, we had technical difficulties due to the COVID-19 pandemic. (*e.g.*, prolonged ordering processes of RT-qPCR reagents, primers, pipette tips, plates, and other consumables due to stock shortage at the manufacturers, and we were not able to irradiate the cell cultures because the visit of the Dept. of Oncotherapy was not allowed for an extended period). Moreover, we also had financial difficulties due to high inflation caused by the Ukrainian war. Therefore, the *in vitro* transfection and validation experiments are ongoing in collaboration with our Austrian partners (Dr. Attila Kiss, Dr. Péter Pokreisz, and Prof. Dr. Bruno K. Podesser, Ludwig Boltzmann Institute for Cardiovascular Research at Center for Biomedical Research and Translational Surgery, Medical University of Vienna, Vienna, Austria).

#### **4.5. Validation of the results of the chronic *in vivo* experiments by miR-modulators in mice (Task 5)**

Chronic mouse models of RIHD were set up with 6, 12, and 18 Gy selected heart irradiation and 24 weeks FUP time. The 18 Gy irradiation dose caused 67% lethality due to severe heart failure. The 6 or 12 Gy RT groups were appropriate RIHD models to test miR modulators or other agents in murine experiments. Based on the NGS and RT-qPCR data, the pro-fibrotic-miR-21-5p, pro-senescent miR-34a-5p, pro-inflammatory miR-223-3p and the oxidative-stress associated miR-383-5p were up-regulated in rats in more FUP time points (1 and/or 3, and/or 19 weeks). Therefore, the antagomiR-21-5p, antagomiR-34a-5p, antagomiR-223-3p, and antagomiR-383-5p seemed to be ideal candidates to ameliorate the severity of RIHD *in vivo*. In contrast to our results, Zhang *et al.* recently found that miR-223-3p protected against radiation-induced cardiac toxicity by alleviating myocardial oxidative stress and programmed cell death via targeting the AMPK pathway (Front. Cell Dev. Biol., 2022, <https://doi.org/10.3389/fcell.2021.801661>). Unfortunately, miR-383-5p seems to be a tumor-suppressor miR in human cancer, therefore its blocking might cause tumor growth (Jafarzadeh et al., Front Cell Dev Biol. 2022; 10: 955486., doi: <https://doi.org/10.3389/fcell.2022.955486>). Therefore, antagomiR-21-5p and antagomiR-34a-5p remained our primary candidates in further *in vivo* experiments (Guo et al., Biochemistry, Biophysics and Molecular Biology, 2020, doi: <https://doi.org/10.7717/peerj.10502>; Hua et al., Front Cardiovasc Med., doi: <https://doi.org/10.3389/fcvm.2021.784044>). Similarly to the *in vitro* transfection experiments, the COVID-19 pandemic and the inflation caused by the war created technical and financial barriers (due to the high price of the adenoviral vector-based antagomiR experiments) to finish this task in time. We plan to finish our experiments with the antagomiR-34a-5p in our mice 12 Gy RIHD model in collaboration with our Austrian partner (Dr. Attila Kiss, Dr. Péter Pokreisz, and Prof. Dr. Bruno K. Podesser, Ludwig Boltzmann Institute for Cardiovascular Research at Center for Biomedical Research and Translational Surgery, Medical University of Vienna, Vienna, Austria).

## **5. Research infrastructure and participants**

The irradiation of animals and cells was performed in the Dept. of Oncotherapy, Albert Szent-Györgyi Medical School, University of Szeged, Hungary, involving Prof. Dr. Zsuzsanna Kahán, Dr. Zoltán Varga, and Dr. Gabriella Fábián. Further animal and cell culture experiments, RT-qPCR, Western blot, and other molecular measurements were mainly performed in the Department of Biochemistry, Albert Szent-Györgyi Medical School, University of Szeged. The participants listed originally in the funding contract were involved in these research activities (Dr. Mónika Gabriella Kovács, Ilona Ungi [technician until 2020], and Dr. Fanni Magdolna Márványkövi [medical student until 2021, then PhD

student]) participated mainly in the *in vivo*, RT-qPCR and WB experiments, Dr. Renáta Molnár-Gáspár, Petra Diószegi (PhD student until 2020, then researcher until 2022), Márton Szabó, and Dr. Dóra Halmi (medical student until 2021, then PhD student) participated the *in vitro* experiments in H9c2 cardiomyoblasts, Dr. Tamás Csont consulted on the preliminary results). Ilona Ungi changed her workplace in 2020; then other technicians (Réka Somogyi, Dóra Csóré, Éva Plechl, and Atina Colic) were involved and gave technical support mainly in the molecular measurements and cell culture experiments. Particularly, Dr. Gergő Szűcs postdoctoral researcher (*in vivo* and Western blot experiments) and 4 PhD students, Dr. Zsuzsanna Kovács (*in vivo* and Western blot experiments, Marah Freiwan (RT-qPCR and Western blot experiments, Dr. Barbara Erdélyi-Furka (*in vitro* experiments in H9c2 cardiomyoblasts, medical student until 2022, then PhD student) and Hoa Dinh Thi Thanh (RT-qPCR experiments) helped the project. Histology stainings were performed with the help of Krisztián Daru, Dr. Bence Kővári, and Prof. Dr. Gábor Cserni. The medical students listed originally in the funding contract (Vivien Csitkovics, Dalma Dajka, Nóra Ágnes Kiss, and Róbert Kovács), participated mainly in the animal experiments until their graduation in 2019-2020. From 2019-2020, new medical students (Réka Losonczy, Merse Kis, Klaudia Kupecz, and Dávid Volford) were involved in the *in vivo* and RT-qPCR experiments and defended their diploma thesis based on the topics of the present grant in 2023.

Petra Diószegi changed her workplace in 2022. After her successful PhD defense, Dr. Mónika Gabriella Kovács started to work at the Department of Internal Medicine and Oncology, Semmelweis University, Budapest, Hungary in September 2022, however, she is still helping us with data analysis and manuscript writing. Dr. Bence Kővári changed his workplace in 2020, however, he helped in the analysis of the histologic slides in the remaining part of the project. In summary, it did not interfere with the execution of the tasks of the present project that 3 researchers changed their workplace.

The hematoxylin-eosin-stained slides were also analyzed by the Biology Image Analysis Software (BIAS) developed by Ferenc Kovács, András Kriston, and Dr. Péter Horváth (Single-Cell Technologies Ltd and Dept. of Biochemistry, Synthetic and Systems Biology Unit, Biological Research Centre, Szeged, Hungary) who allowed us to use their software before its public release. Xenovea Ltd. performed NGS and the bioinformatic analysis, and proteomics measurements and analysis were performed in the Dept. of Medicinal Chemistry, Albert Szent-Györgyi Medical School, University of Szeged in collaboration with Bella Bruszel and Dr. Zoltán Szabó. Several laboratory parameters in blood plasma samples were measured in the Dept. of Laboratory Medicine, Albert Szent-Györgyi Medical School, University of Szeged, in collaboration with Dr. Andrea Siska, Katalin Farkas, and Imre Földesi. The cell culture experiments in human breast cancer lines were performed in collaboration with Dr. Renáta Minorics, Prof. Dr. István Zupkó (Institute of Pharmacodynamics and Biopharmacy, Faculty of Pharmacy, University of Szeged, Hungary), and with the help of a shared MSc student, Szonja Polett Pósa. The cell culture experiments in human ventricular cardiac fibroblasts were performed in collaboration with Dr. Attila Kiss, Dr. Péter Pokreisz, and Prof. Dr. Bruno K. Podesser, Ludwig Boltzmann Institute for Cardiovascular Research at Center for Biomedical Research and Translational Surgery, Medical University of Vienna, Vienna, Austria. Several preliminary RT-qPCR experiments were performed at the IMTTS, Hannover Medical School, Germany, in collaboration with Dr. Sándor Bátkai and Prof. Dr. Thomas Thum, and at the Biological Research Centre, Szeged, Hungary, in collaboration with Dr. Ágnes Zvara and Prof. Dr. László Puskás.

In the summer of 2023, the PI was given the opportunity to establish a new cardiovascular research group at the Department of Pathophysiology, Albert Szent-Györgyi Medical School, University of Szeged. Her former medical students (Réka Losonczy, Merse Kis, Klaudia Kupecz, and Dávid Volford) joined the new group as Ph.D. students and are working on onco-cardiology topics related to the results of the present project under the supervision of the PI from September 2023.

## 6. Summary of the scientific output

During the supportive period of the project, we have published 9 *in extenso* articles in internationally recognized scientific journals (all are open access articles, 8 of them are D1 and 1 is Q1

according to SJR, 5 are related to the topics of present project and the other 4 articles hold the present grant ID). The cumulative impact factor of these publications is over 55 and their citation is approximately 100 in the last 5 years according to Google Scholar (IF of the 5 articles related to the present project is approximately 27 and their citation is over 80; and IF of the other 4 articles is approximately 30 and their citation is 18). We plan to submit 3 new original research manuscripts (results on PIF, NGS, and proteomics data) within one year based on the findings of the present project. We also plan to write a methodologic book chapter on the set-up of RIHD models in rodents and further original manuscripts and review articles related to the present project in the long term.

Beyond the scientific publications and the PhD defenses, the results of this project were already used in 8 diploma theses (Nóra Kiss, Róbert Kovács, Vivien Csitkovics, Barbara Erdélyi-Furka, Réka Losonczi, Merse Kis, Klaudia Kupecz, and Dávid Volford). The results were also shown in the forms of poster (6) and oral presentations (9) at national and international scientific conferences as well as local (11) and national (9) undergraduate research (TDK) conferences (we collected 2 first and 2 second prizes related to the RT- and doxorubicin-induced cardiotoxicity topics at the national (OTDK) conferences). Unfortunately, the COVID-19 pandemic and the inflation caused by the Ukrainian war slowed down the experiments and the scientific output of this project (*e.g.*, COVID infections, PhD students and undergraduate students were prohibited from visiting the buildings of the University of Szeged, and the Dept. of Oncotherapy was also unreachable to continue the irradiations; extraordinary slow purchasing and administration processes, significantly increased prices of consumables due to the inflation).

In summary, we consider our project a successful one despite all of the difficulties, and this grant's financial support helped us reach our scientific and personal goals. We hope that our present pre-clinical results might open new horizons in drug development against diastolic dysfunction and pathologic cardiac remodeling in RIHD in the future.